REFERENCES

1. R. Pichoir, in "Materials and Coatings to Resist High Temperature Corrosion," D. R. Holmes and A. Rahmel, Editors, p. 271, Applied Science Publishers, London (1978).
2. P. N. Walsh, in "Chemical Vapor Deposition," G. F. Wakefield and J. B. Blocker, Editors, p. 147, The Electrochemical Society Softbound Proceedings Series, Princeton, NJ (1973).
3. S. R. Levine and R. M. Caves, *This Journal*, **121**, 1051 (1974).
4. L. L. Seigle, B. K. Gupta, R. Shankar, and A. K. Sarkhel, NASA Contract Report 2939, prepared for Lewis Research Center under Contract NGR-33-016-160, NASA Scientific and Technical Information Office (1978).
5. R. A. Rapp, D. Wang, and T. Weisert, in "Metallurgical Coatings," M. Khobaib and R. Krutenat, Editors, p. 131, TMS-AIME, Warrendale (1987).
6. D. C. Tu and L. L. Seigle, *Thin Solid Films*, **95**, 47 (1982).
7. R. Sivakumar and L. L. Seigle, *Met. Trans.*, **13A**, 495 (1982).
8. B. K. Gupta, A. K. Sarkhel, and L. L. Seigle, *Thin Solid Films*, **39**, 313 (1976).
9. B. K. Gupta and L. L. Seigle, *ibid.*, **73**, 365 (1980).
10. N. Kandasamy, F. J. Pennisi, and L. L. Seigle, *ibid.*, **84**, 17 (1981).
11. S. R. Adolph, M.S. Thesis, Department of Materials Science & Engineering, State University of New York, Stony Brook, New York (1983).
12. G. J. Marijnissen, H. V. Gameren, and J. A. Klostermann, in "High Temperature Alloys for Gas Turbines," D. Coutsouradis, P. Felix, H. Fischmeister, L. Habraken, Y. Lindblom, and M. O. Speidel, Editors, p. 231, Applied Science, London (1978).
13. B. Nciri and L. Vandenbulke, *Surf. Technol.*, **24**, 365 (1985).
14. B. Nciri and L. Vandenbulke, *J. Less-Common Metals*, **95**, 55 (1983).
15. B. Nciri and L. Vandenbulke, *ibid.*., **95**, 191 (1983).
16. G. Eriksson, *Chem. Scr.*, **8**, 100 (1975).
17. W. R. Daisak and N. Kandasamy, Work in progress in the Dept. of Materials Science, State University of New York, Stony Brook, NY.
18. J. Eldridge and K. L. Komarek, *Trans. Metall. Soc. AIME*, **230**, 226 (1964).
19. J. I. Goldstein, D. E. Newbury, P. Echlin, D. C. Joy, C. Fiori, and E. Lifshin, "Scanning Electron Microscopy and X-Ray Microanalysis," Plenum Press, New York (1981).
20. G. Eriksson and E. Rosen, *Chemica Scripta*, **4**, 193 (1973).
21. K. Schwerdtfeger and E. T. Turkdogan, in "Physicochemical Measurements in Metals Research," Vol. IV, part 1, R. A. Rapp, Editor, p. 380, Interscience Publisher, New York (1970).
22. J. O. Herschfelder, R. B. Bird, and E. L. Spotz, *Chem. Rev.*, **44**, 205 (1949).
23. J. O. Hirschfelder, C. F. Curtiss, and R. B. Bird, "Molecular Theory of Gases and Liquids," John Wiley and Sons, Inc., New York (1951).
24. N. Wakao and J. M. Smith, *Chem. Eng. Sci.*, **17**, 825 (1962).
25. K. Nishida, T. Yamamoto, and T. Nagatta, *Trans. Jpn. Inst. Met.*, **12**, 310 (1971).
26. F. Lihl and H. Ebel, *Arch. Eisenhuttenw*, **32**, 483 (1961).

Chemical Stability of Sodium Beta″-Alumina Electrolyte in Sulfur/Sodium Polysulfide Melts

Meilin Liu and Lutgard C. De Jonghe

Materials and Chemical Science Division, Lawrence Berkeley Laboratory and Department of Materials Science and Mineral Engineering, University of California, Berkeley, California 94720

ABSTRACT

Immersion of sodium β″-alumina electrolyte in sodium polysulfide and pure sulfur melts, at Na/S battery operation temperatures, showed that the electrolyte was chemically attacked by the melts, and that the extent of degradation was affected by a number of factors, including surface morphology and chemistry of the electrolyte, melt composition, impurity contamination, etc. The corrosion reactions mostly initiated and concentrated on defected areas, and were catalyzed by the presence of impurities such as water, moist air, oxygen, etc. The corrosion power of sodium polysulfide melts increased with the sulfur content in the range of Na_2S_2 to Na_2S_5. The reaction products, formed at the interface, were believed to be Na_2SO_4, $NaAl(SO_4)_2$, $Al_2(SO_4)_3$, $NaHSO_4$, Na_2CO_3, NaOH, etc. Precipitation of crystallized sulfates occurred on preferred areas after saturation. Corrosion products of transition metals also deposited on the electrolyte surface. As a result, a partly insulating layer was formed on the electrolyte surface during immersion, which was a mixture of sulfates, carbonates, and sulfides of transition metals.

Degradation of the β″-electrolyte is one of the important limitations which determine whether or not Na/S batteries may be useful for energy storage and conversion systems. There has been considerable effort in establishing the mechanism of degradation of the electrolyte in contact with the negative electrode (liquid sodium) (1). De Jonghe *et al.* have reported the degradation of the electrolyte in contact with the positive electrode (sulfur/sodium polysulfide melts) (2), but much remained unknown concerning the nature of the electrolyte/polysulfide melt interface. Recently, Choudhury made an assessment of thermochemical stability of β- and β″-alumina electrolytes in pure sulfur with carbon (3). In the present paper, the degradation of the electrolyte in various environments, in different melt compositions (from Na_2S_2 to Na_2S_5 to pure sulfur), with or without impurity contamination (water, moist air, oxygen, cell case material, and carbon), are reported and the reactions between the solid electrolyte and the melts under these conditions were proposed based on thermodynamic estimations.

Experimental

Materials.—Polysulfides.—Four different polysulfides, Na_2S_2, Na_2S_3, Na_2S_4, and Na_2S_5, and pure sulfur were used. The pure sulfur was obtained from the Lawrence Livermore Laboratory. The disulfide Na_2S_2 was prepared from the monosulfide Na_2S (from NAOH Chemicals) and from pure sulfur in our laboratory, in a dry box (oxygen- and water-free to less than 1 ppm). After the pure sulfur was dried in the dry box for 3 days, the appropriate amounts of Na_2S and dry sulfur powders were mixed and put in a quartz tube, sealed at about 10^{-2} torr, and then slowly heated to 750°C to form Na_2S_2. The Na_2S_2 was cooled to room temperature and transferred to glass test tubes within the dry box. The Na_2S_3 was obtained from Brown-Boveri and Cie (BBC) and stored in vacuum. The Na_2S_4

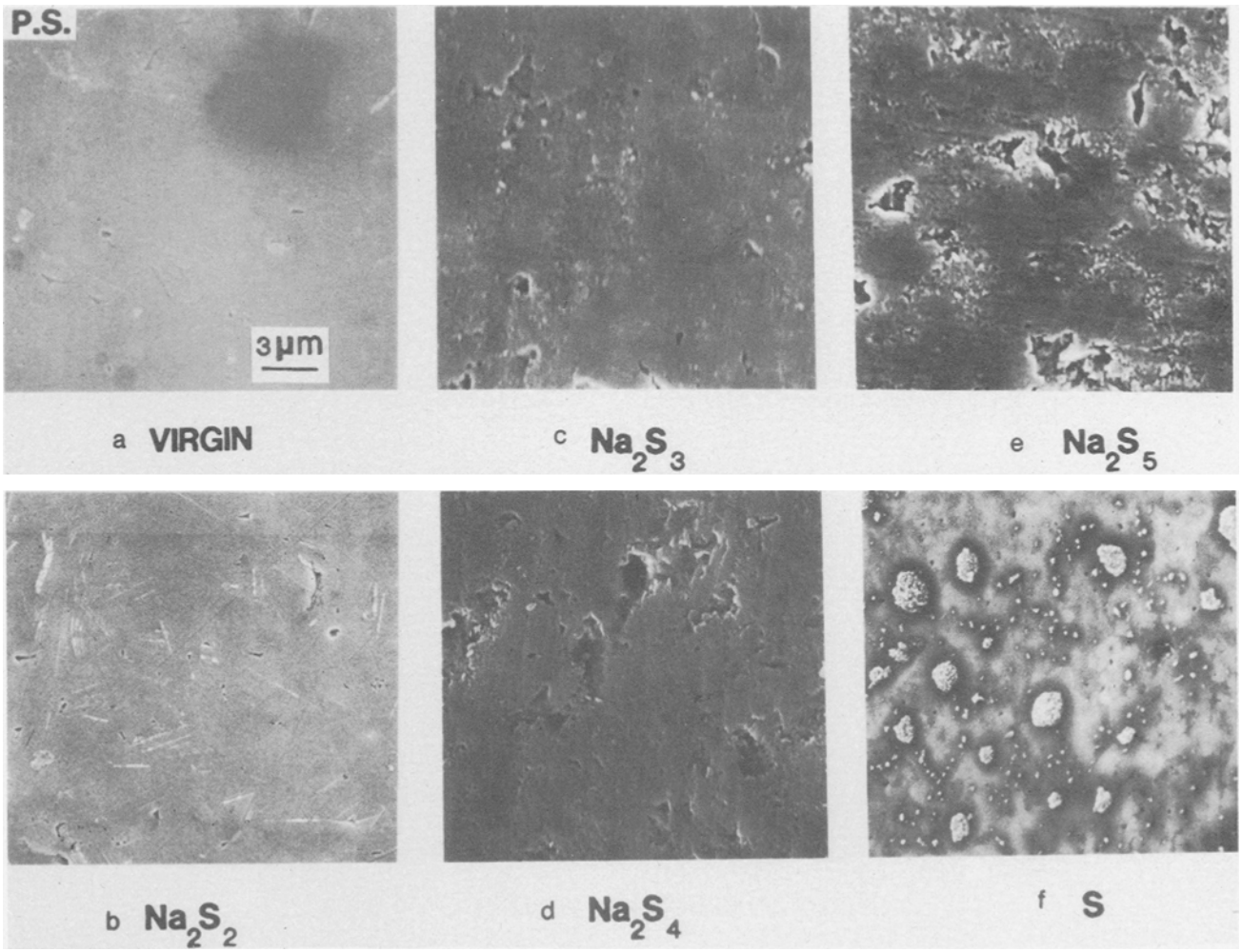

Fig. 1. Scanning electron micrographs of the polished surface of the electrolyte before and after five week immersion in sodium polysulfide melts with different compositions. (a) As-polished before immersion; (b) immersed in Na_2S_2 (350°C); (c) in Na_2S_3 (400°C); (d) in Na_2S_4 (400°C); (e) in Na_2S_5 (400°C); (f) immersed in pure sulfur (350°C).

was prepared by Dow Chemicals Company and stored in the dry box. Na_2S_5 was made from mixtures of either Na_2S_3 or Na_2S_4 with pure sulfur.

β″-Alumina electrolyte.—The polycrystalline electrolyte consisted of bars with approximate dimensions of 45 × 10 × 4 mm, and was prepared by Ceramatec of Salt Lake City, Utah (4). The chemical composition given by the manufacturer was 8.85 weight percent (w/o) Na_2O, 0.7 w/o Li_2O, balance Al_2O_3.

Specimen preparation.—Two different surfaces—polished and as-sintered—were examined to determine how the surface morphology affects the stability of the electrolyte. Specimens were sectioned with a diamond saw, ground with α-Al_2O_3 and polished to a 1 μm diamond finish (Fig. 1a). Even though the polished surfaces were very smooth, some imperfections, such as cavities and large grains still remained. Mechanical damage, including microcracks, may also be produced during polishing. As-sintered surfaces are shown in Fig. 2a. Some workers have reported that these surfaces might be covered by a thin, glassy film, which would be formed during sintering (5). Specimens have different surface morphologies were washed with methyl alcohol in an ultrasonic cleaner, and then heated up to 800°C for 12h to drive off absorbed water.

Impurity contamination.—Water.—Electrolyte specimens were either exposed to 100% relative humidity or immersed in distilled water at room temperature for one week (168h) to pick up water. Then, the surface water was removed by heating the specimens at 100°C for 5 min.

Oxygen.—After vacuum-drying and before sealing, oxygen gas was put into the test tubes to build up an oxygen atmosphere of about 100 torr.

Moist air.—The dried electrolyte was exposed to atmosphere (moist air) at room temperature for 1 week (168h).

Fe-Ni-Cr and C.—Cell container materials (stainless steel) and current collector material (graphite felt) were put in with some polysulfide powders, before sealing the glass capsules.

Procedures.—Because of the sensitivity of polysulfides to moisture, the test must be set up in a water and oxygen free glove box. Specimens and polysulfides were put into glass test tubes in the dry box and sealed under mechanical vacuum. The sealed tubes were placed vertically in a box furnace at the desired temperatures (350° or 400°C). After the specimens had been kept in molten polysulfides for the desired period (5 or 10 weeks), the glass tubes were cooled to room temperature and broken. The specimens were removed, ultrasonically cleaned in methyl alcohol, and dried, before characterization and analysis. Specimens immersed in sulfur were cleaned in CS_2.

Results

Morphological characterization.—Effect of composition.—Figures 1 and 2 show the changes in surface morphology of electrolytes before and after 5 week immersion in melts with compositions of Na_2S_3, Na_2S_4, and Na_2S_5, at 400°C, and Na_2S_2 and pure sulfur at 350°C.

The surfaces of polished specimens are shown in Fig. 1. Very little has happened to the polished surface immersed in Na_2S_2 and Na_2S_3 melts. However, on the polished surface in the Na_2S_4 melt, some compounds formed on areas containing defects such as microcracks, pores, etc., which were introduced by mechanical polishing. On the polished surface immersed in Na_2S_5, a nonuniform and discontinuous, thin surface layer was formed and more corrosion

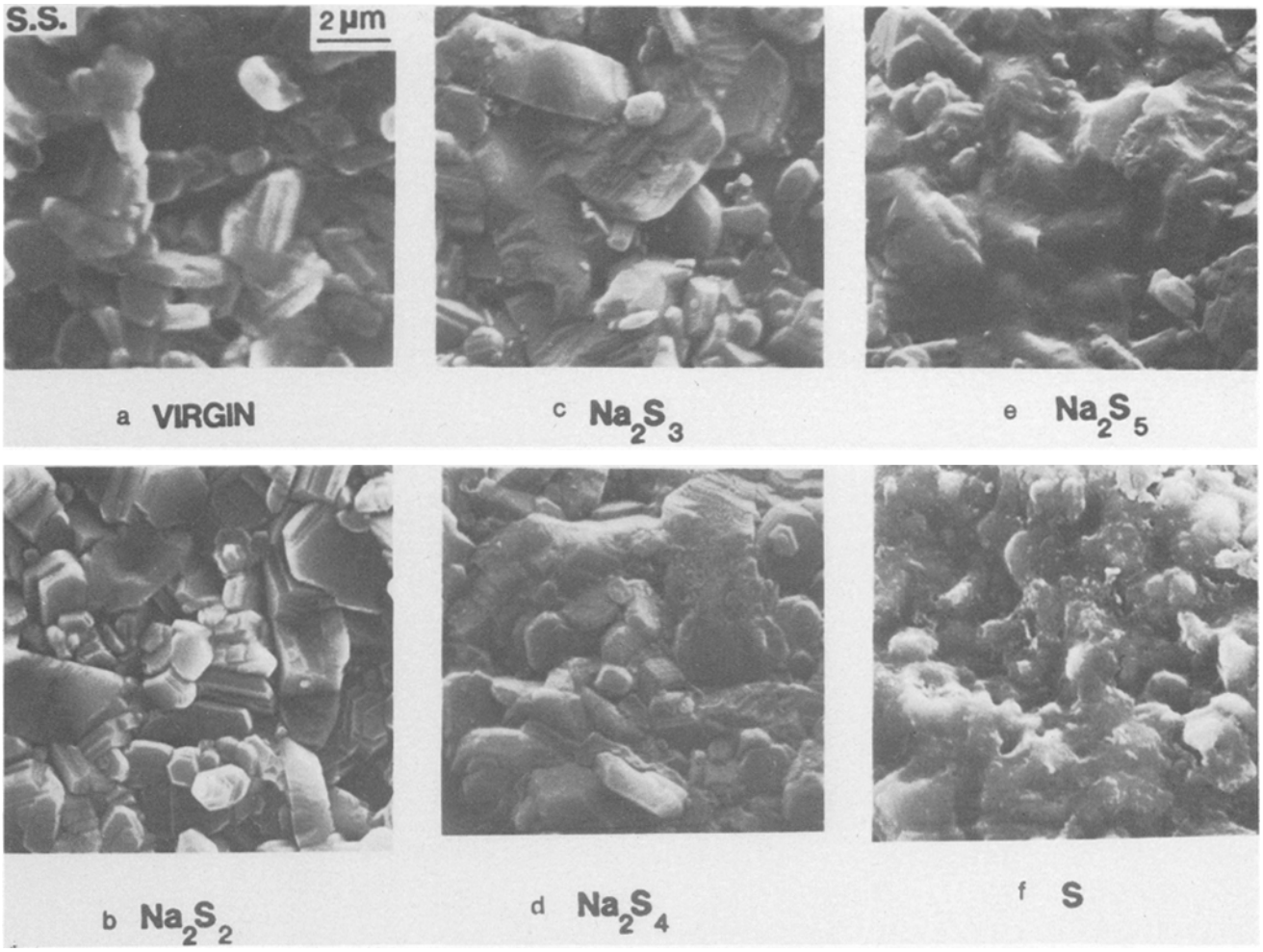

Fig. 2. Sintered surfaces of the electrolyte (same experimental conditions and arrangement as in Fig. 1)

products were evident at areas containing flaws or irregularities (Fig. 1e). The changes in surface morphology were even more pronounced for the samples immersed in pure sulfur, where the surface was completely covered by a corrosion layer (Fig. 1f).

The surfaces of sintered electrolytes are shown in Fig. 2. After immersion, the surfaces were covered with a thin product layer, while some compounds had accumulated in the surface pores. The extent of the reactions apparently increased from Na_2S_2 to Na_2S_5 to pure sulfur.

Effect of impurity contamination.—Figures 3 and 4 show the changes in morphology of polished and sintered surfaces before and after immersion at 400°C for 5 weeks in Na_2S_3 with the presence of oxygen, water, moist air, or stainless steel (Fe-Ni-Cr) plus graphite felt (C). An Na_2S_3 melt was chosen because, without impurities, this melt was among the least reactive ones, as shown in Fig. 3b and 4b. However, in the presence of impurities, the change in surface morphology and chemistry can be dramatic.

Steel + carbon (Fig. 3c and 4c).—The presence of transition metals and graphite felt considerably affected the interaction between the Na_2S_3 melt and the electrolyte. A corrosion product layer covered the entirety of the surface, and some octahedrally shaped crystals had formed.

Oxygen (Fig. 3d and 4d).—The effects of the presence of oxygen contamination on the Na_2S_3/electrolyte system are: (*i*) creation of a corrosion layer on most of the areas of the polished surfaces (Fig. 3d); (*ii*) considerable acceleration of the reactions and increase of the deposition of corrosion products; and (*iii*) precipitation of crystallized compounds on the sintered surface in addition to the overall thin product layer that formed without oxygen present.

Water (Fig. 3e and 4e).—In the case of absorption of water in electrolytes, there is an obvious etching effect: the grain boundaries are clearly revealed and the altered surface topology indicates chemical attack. Some corrosion products had been deposited between grains.

Moist air (Fig. 3f and 4f).—The exposure of the electrolyte to moist air (H_2O, O_2, CO_2, etc.) had the combined effects of water and oxygen contamination.

Time dependence.—Figures 5 and 6 show the changes in surface morphology of electrolytes before and after immersion for 5 and 10 weeks in molten Na_2S_5, at 400°C. This composition was chosen in this case because Na_2S_5 is the most corrosive of the sodium sulfides and hence would make the differences most obvious as immersion time increased if the corrosion were time dependent.

Polished electrolytes (Fig. 5).—Figure 5a shows the surface of an as-polished electrolyte before immersion. Five weeks later, some corrosion compounds are nonuniformly distributed, and most of them are concentrated around imperfections (Fig. 5b). After 10 weeks, a uniform compound layer, covering the whole surface, had formed and some precipitation had occurred, leading to groups of plate-shaped crystallites (Fig. 5c). The high magnification micrograph (Fig. 5d) shows that the layer is porous but not entirely uniform: more corrosion products had accumulated in defect areas.

Sintered electrolytes (Fig. 6).—A comparison with virgin materials clearly indicates that a compound layer, covering the entire surface, was well established after 5 weeks immersion with some crystals just starting to grow (Fig. 6b). However, many more new crystals and compounds, formed at grain junctions, were found on the surface after 10 weeks immersion (Fig. 6c and 6d). An even higher magnification micrograph (Fig. 6e) shows the detailed morphology of the flower-shaped crystal clusters and the thin layer. The thin layer looks porous and developed deeper in

the defected areas where precipitation of crystallized corrosion products apparently had occurred.

Chemical characterization.—An Auger electron spectrum obtained from a polished surface of samples immersed in the Na_2S_5 melt for 10 weeks is shown in Fig. 7a. The elements present in the spectrum should represent the average composition of corrosion compounds. Figure 7b shows the profile of the impurities in the degraded layer at different sputtering time. The quantity of sulfur decreases as sputtering time increases, clearly indicating that a reaction or corrosion layer had formed on the electrolyte surface. This layer was sputtered off in 10 min. The sulfur probably was present as sulfates because a large quantity of oxygen was also detected at the same time. Attempts to identify the corrosion compounds by x-ray diffraction were unsuccessful.

Discussion

Experimental observations indicated that the electrolyte reacts chemically with Na_2S_x melts. To identify possible reactions at the electrolyte/melt interface, thermodynamic estimations were performed.

Thermodynamic considerations.—The β″-alumina electrolyte investigated in the experiment has a chemical composition of $(0.86Na_2O \cdot 0.14Li_2O) \cdot 5.34Al_2O_3$, with some β-phase. As a reasonable approximation, the formula $Na_2O \cdot yAl_2O_3$ is used to represent the majority β″-phase, with $y = 5.34$, and the minoriy β-phase with $y = 8$. The data on the Gibbs free energy of formation of an electrolyte with composition of $Na_2O \cdot 8Al_2O_3$, obtained by Weber with electrochemical methods and calculated by Kummer (6), are used for the β-phase. These data were evaluated for high temperatures, and extrapolated to temperatures around 300°-400°C. The approximate Gibbs free energy of formation of the β″-phase was based on the data for the β-phase and the Na_2O activities in β- and β″-alumina, as reported by Itoh (7). The Gibbs free energies of formation of sodium polysulfides were calculated by Gupta (8) from open-circuit cell voltage measurements. Other data were obtained from the NBS tables of chemical thermodynamic properties (9) and from the JANAF thermochemical tables (10). The Al_2O_3 released in the reactions is assumed to be α-Al_2O_3, as proposed by Choudhury (3).

Based on these thermodynamic data (Table I) and the assumptions, the standard Gibbs free energies for the reactions between the solid electrolyte and sulfur/sodium polysulfide melts are estimated from

$$\Delta_r G^\circ = \sum_i (\nu_i \cdot \Delta_f G^\circ)_{(\text{product})} - \sum_i (\nu_i \cdot \Delta_f G^\circ)_{(\text{reactant})} \quad [4.0]$$

The chemical reactions that could occur on the surfaces of the electrolyte are postulated as follows

1. Reactions between pure sulfur and the solid electrolyte

$$Na_2O \cdot yAl_2O_3 + \frac{(3x+1)}{4} S \rightarrow \frac{3}{4} Na_2S_x + \frac{1}{4} Na_2SO_4 + yAl_2O_3 \quad [4.1a]$$

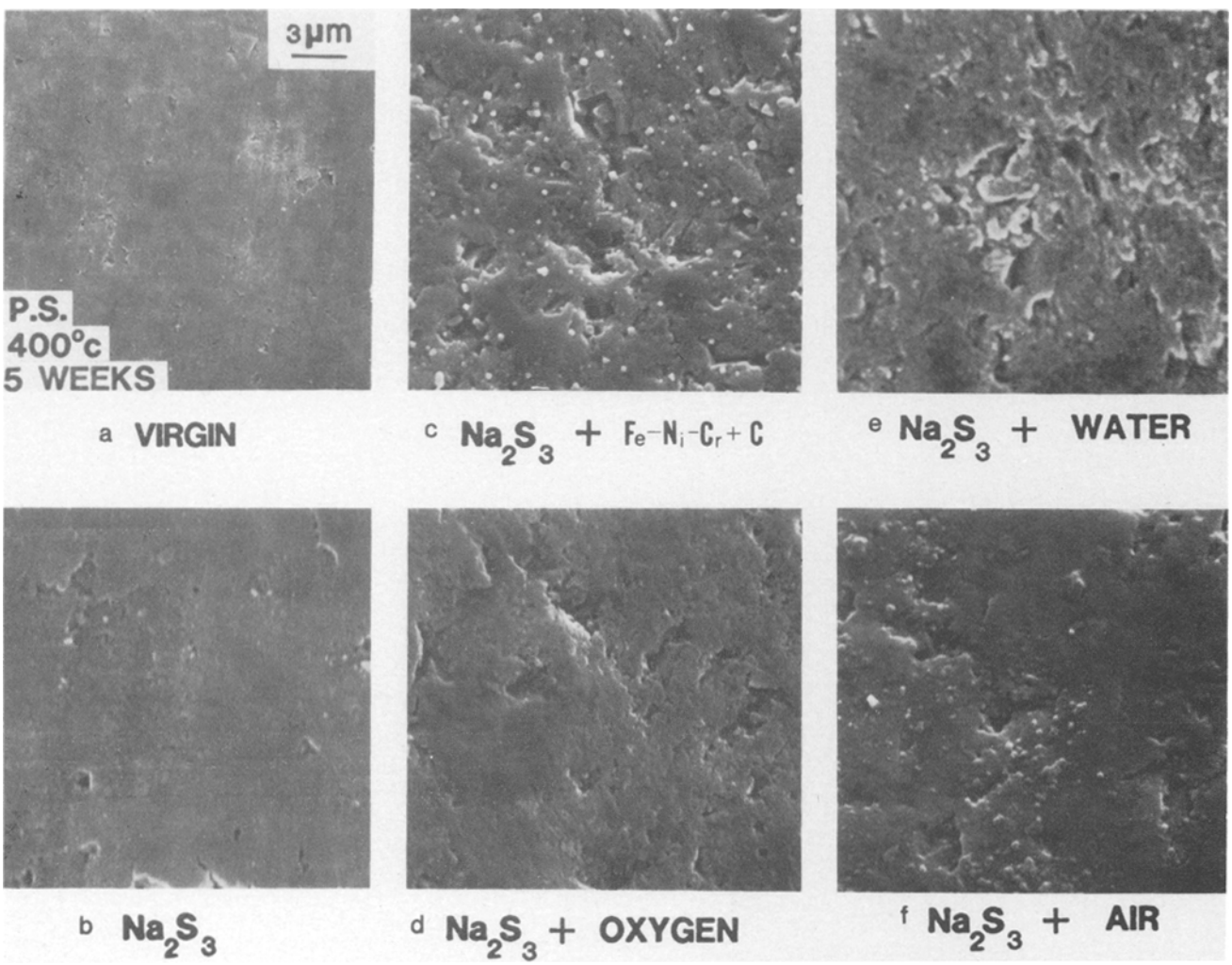

Fig. 3. SEM micrographs of the polished surfaces of the electrolyte before and after five week immersion, at 400°C, in Na_2S_3 melts, with or without impurity contamination. (a) As prepared before immersion; (b) dry, uncontaminated samples immersed in pure Na_2S_3 (without impurity contamination); (c) dry samples immersed in Na_2S_3 with stainless steel (Fe-Ni-Cr) and graphite felt (C); (d) dry samples immersed in Na_2S_3 melt with an oxygen atmosphere of about 100 torr; (e) wet samples immersed in Na_2S_3 melt; (f) samples exposed to moist air for one week before immersion.

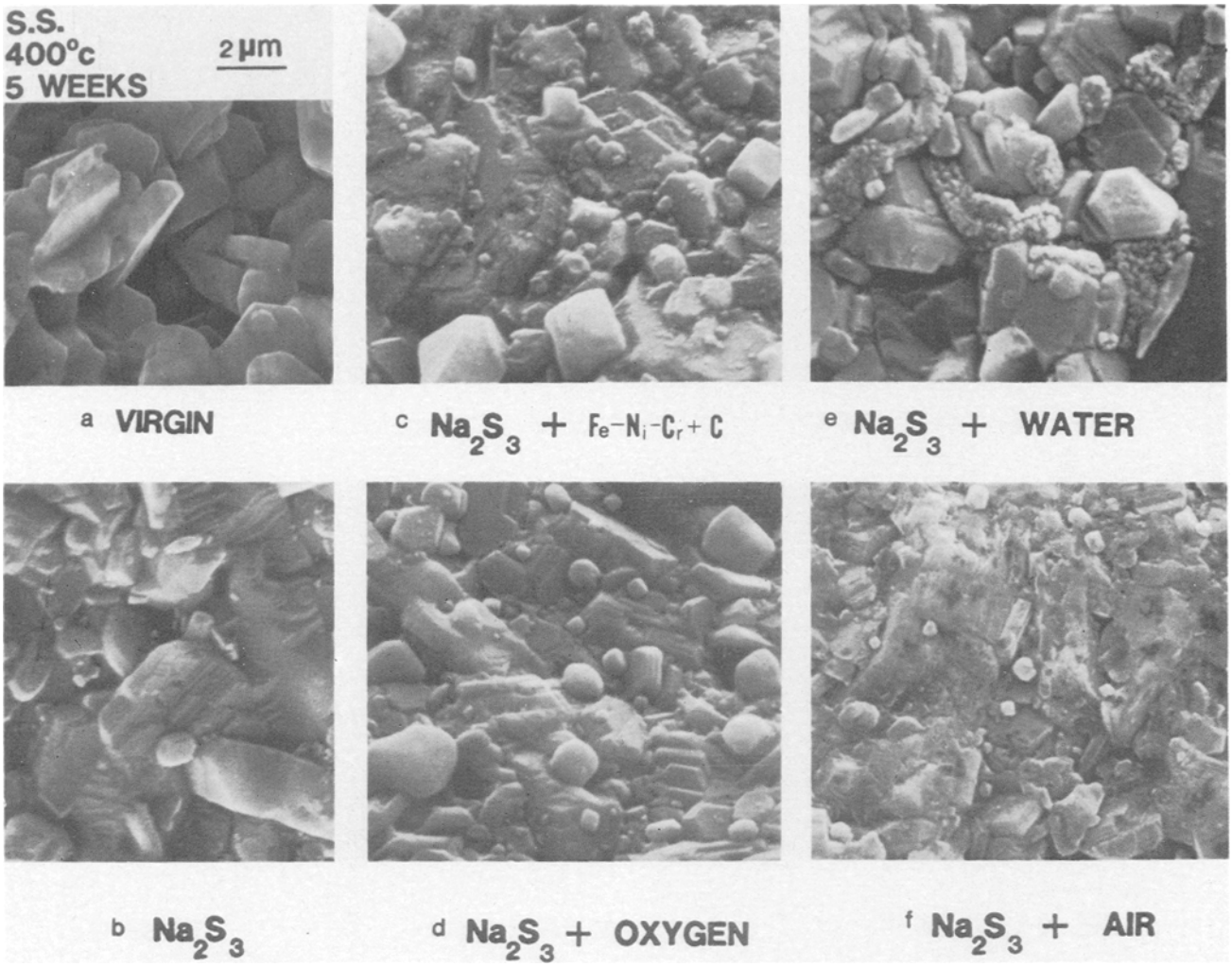

Fig. 4. Sintered surfaces of the electrolyte (same experimental conditions and arrangement as in Fig. 3)

$$Na_2O \cdot yAl_2O_3 + \frac{(3x+1)}{3} S \rightarrow Na_2S_x + \frac{1}{9} Al_2(SO_4)_3 + \left(y - \frac{1}{9}\right) Al_2O_3 \qquad [4.1b]$$

$$Na_2O \cdot yAl_2O_3 + \frac{(12x+4)}{13} S \rightarrow \frac{2}{13} NaAl(SO_4)_2 + \frac{12}{13} Na_2S_x + \left(y - \frac{1}{13}\right) Al_2O_3 \qquad [4.1c]$$

When excess sulfur is available, as is the case when the electrolyte is immersed in a sulfur melt, only Na_2S_5 may form in the above reactions; however, Na_2S_x with x less than five might form when the amount of sulfur available is limited, as during charging a Na/S battery.

The chemical reactions between the electrolytes and pure sulfur proposed by Choudhury (3) produce corrosion products Na_2SO_3, Na_2SO_4, SO_2, and O_2. Our estimation indicates, however, that the thermodynamically stable corrosion products are Na_2SO_4, $Al_2(SO_4)_3$, $NaAl(SO_4)_2$, etc., because SO_2/SO_3 and O_2 can react further to produce sulfates. The formation of SO_2 and $NaSO_3$ is possible, but the formation of SO_3 and Na_2SO_4 appears more favorable thermodynamically.

2. Reactions between Na_2S_x and the solid electrolyte

$$Na_2O \cdot yAl_2O_3 + \frac{(3x-2)}{4} Na_2S_x \rightarrow \frac{1}{4} Na_2SO_4 + \frac{(3x+1)}{4} Na_2S_{(x-1)} + yAl_2O_3 \qquad [4.2a]$$

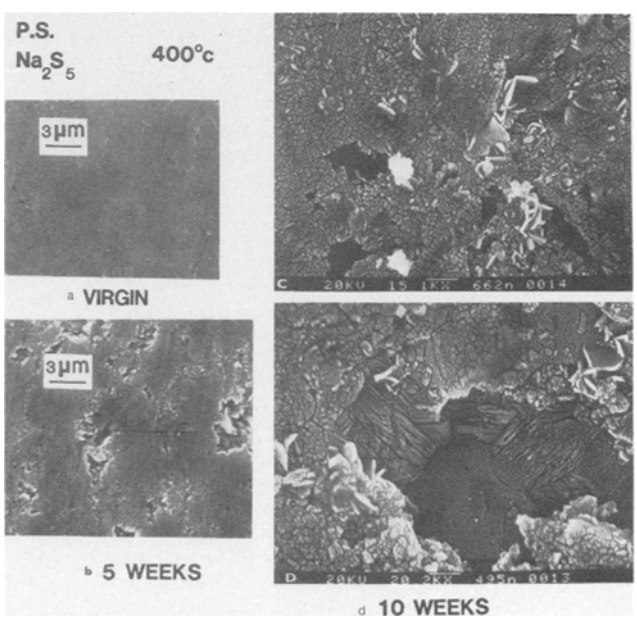

Fig. 5. SEM micrographs of the polished surfaces of the electrolyte immersed in pure Na_2S_5, at 400°C, for different periods of time. a, Virgin material as prepared before immersion; b, five week immersion; c, ten week immersion; d, a high magnification micrograph showing the detailed surface morphology after ten week immersion.

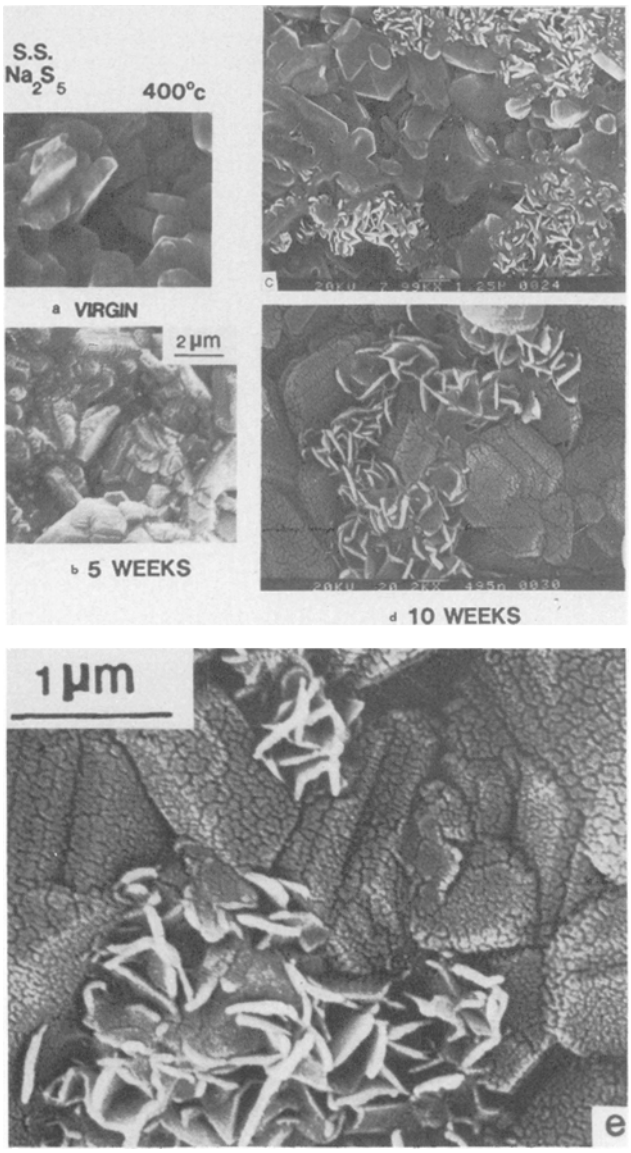

Fig. 6. Sintered surfaces of the electrolyte (same experimental conditions and arrangement as in Fig. 5). Fig. 6e is a high magnification SEM micrograph showing the detailed morphology of the flower-shaped crystal clusters and the degraded layer after 10 week immersion.

$$Na_2O \cdot yAl_2O_3 + \frac{(3x-2)}{3} Na_2S_x \rightarrow \frac{1}{9} Al_2(SO_4)_3 + \frac{(3x+1)}{3} Na_2S_{(x-1)} + \left(y - \frac{1}{9}\right) Al_2O_3 \qquad [4.2b]$$

$$Na_2O \cdot yAl_2O_3 + \frac{4(3x-2)}{13} Na_2S_x \rightarrow \frac{2}{13} NaAl(SO_4)_2 + \frac{4(3x+1)}{13} Na_2S_{(x-1)} + \left(y - \frac{1}{13}\right) Al_2O_3 \qquad [4.2c]$$

The reactions with negative Gibbs free energies, see Table II, are the ones thermodynamically possible, although some may not be fast enough to be significant.

The reaction mechanism could involve at first a partial Na^+ depletion of the electrolyte, described by

$$Na^x{}_{Na}\,(E) = Na^+\,(M) + V_{Na}'\,(E) \qquad [4.3a]$$

where E and M refer to the solid electrolyte and to the melt, respectively

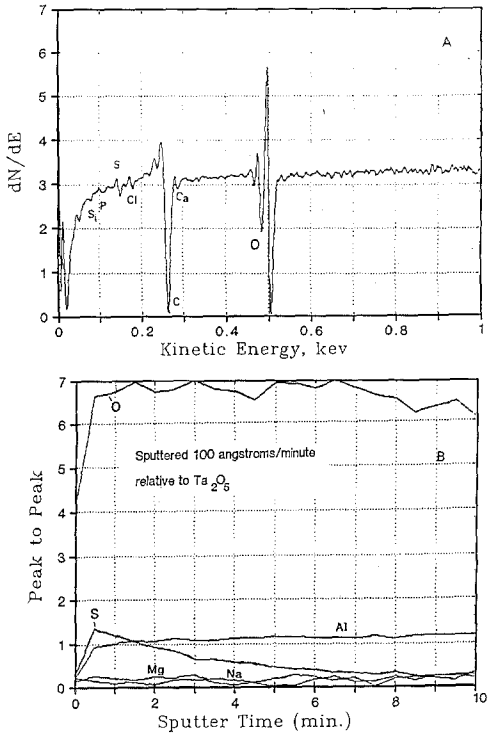

Fig. 7. (A) Auger electron spectrum of a polished surface of the electrolyte after ten week immersion in pure Na_2S_5 at 400°C. The corresponding morphology is shown in Fig. 5 (c) and (d). (B) Profile of the impurities in the degraded (corrosion) layer formed on the electrolyte surface during ten week immersion in pure Na_2S_5 at 400°C (concentration of impurities vs. sputtering time).

$$Na^x{}_{Na}\,(E) + e' + \frac{(x-1)}{2} Na_2S_x\,(M) \rightarrow \frac{x}{2} Na_2S_{(x-1)}(M) + V_{Na}'\,(E) \qquad [4.3b]$$

or

$$Na^x{}_{Na}\,(E) + e' + \frac{x}{2} S\,(M) \rightarrow \frac{1}{2} Na_2S_x\,(M) + V_{Na}'\,(E)$$

Table I. The extrapolated standard Gibbs free energies of formation of the compounds involved in the reactions between the electrolyte and sulfur/sodium polysulfide melts (kcal/mol)

Compound	350°C	400°C	Source
Na_2S_5	−95.8	−95.7	Gupta
Na_2S_4	−95.1	−95.1	
Na_2S_3	−92.7	−92.2	
Na_2S_2	−88.4	87.2	
β-Al_2O_3 (y = 8)	−2,963.9	−2,930.4	Kummer
β″-Al_2O_3 (y = 5.34)	−2,018.9	−1,995.8	Itoh
Na_2S	−80.2	−79.6	JANAF
α-Al_2O_3	−353.9	−350.1	
H_2O	−50.9	−50.3	
CO_2	−94.5	−94.5	
NaOH	−78.4	−77.0	
SO_3	−80.2	−76.5	
H_2S	−10.3	−10.4	
Na_2SO_4	−272.1	−267.4	
Na_2CO_3	−228.4	−225.1	
$Al_2(SO_4)_3$	−700.6	−669.9	[a]
$NaAl(SO_4)_2$	−486.4	−474.2	
$NaHSO_4$	−225.5	−201.7	

[a] Estimated from the relevant data in NBS and JANAF.

Table II. The estimated standard free energies of the reactions between the electrolyte and sulfur/Na_2S_x(M) (without impurity contamination) (kcal/mol)

Equation no.	x as in Na_2S_x	$(\Delta_rG°)_{350°C}$ β $y = 8$	$(\Delta_rG°)_{350°C}$ β″ $y = 5.34$	$(\Delta_rG°)_{400°C}$ β $y = 8$	$(\Delta_rG°)_{400°C}$ β″ $y = 5.34$
Eq. [4.1a]	5	−6.8	−10.5	−9.1	−12.4
	4	−6.3	−10.1	−8.7	−11.9
	3	−4.6	−8.3	−6.5	−9.8
	2	−1.3	−5.0	−2.8	−6.0
	1	4.9	1.1	2.9	−0.3
Eq. [4.1b]	5	−1.3	−5.0	−1.8	−5.0
	4	−0.6	−4.3	−1.2	−4.4
	3	1.8	−2.0	1.7	−1.5
	2	6.1	2.4	6.7	3.5
	1	14.3	10.6	14.3	11.1
Eq. [4.1c]	5	−3.0	−6.7	−4.9	−8.1
	4	−2.4	−6.1	−4.3	−7.6
	3	−0.2	−3.9	−1.7	−4.9
	2	3.8	0.1	3.0	−0.3
	1	11.4	7.6	10.0	6.7
Eq. [4.2a]	5	−4.2	−8.0	−6.8	−10.0
	4	1.4	−2.4	0.7	−2.5
	3	6.3	2.6	6.0	2.8
	2	13.0	9.3	10.5	7.3
Eq. [4.2b]	5	2.2	−1.6	1.4	−1.9
	4	9.7	5.9	11.4	8.2
	3	16.3	12.5	18.4	15.2
	2	25.2	21.5	24.5	21.2
Eq. [4.2c]	5	0.2	−3.6	−2.0	−5.2
	4	7.1	3.4	7.3	4.0
	3	13.2	9.5	13.8	10.5
	2	21.5	17.7	19.3	16.1

Electroneutrality requires that the crystal release the excess oxygen (Eq. [4.3c]). This oxygen can react with Na_2S_x (M) to give SO_3 (Eq. [4.3d])

$$O^x{}_o\,(E) \rightarrow \ddot{V}_o\,(E) + \frac{1}{2}\,O_2\,(M) + 2e' \qquad [4.3c]$$

$$O_2\,(M) + \frac{2}{3}\,Na_2S_x\,(M) \rightarrow \frac{2}{3}\,Na_2S_{(x-1)}\,(M) + \frac{2}{3}\,SO_3\,(M) \qquad [4.3d]$$

The SO_3 can react further to produce corrosion products Na_2SO_4, $NaAl(SO_4)_2$, $Al_2(SO_4)_3$, etc., through the reactions

$$SO_3 + Na_2O \cdot yAl_2O_3 \rightarrow Na_2SO_4 + yAl_2O_3 \qquad [4.3e]$$

$$SO_3 + \frac{1}{4}\,Na_2O \cdot yAl_2O_3 \rightarrow \frac{1}{2}\,NaAl(SO_4)_2 + \frac{(y-1)}{4}\,Al_2O_3$$

$$SO_3 + \frac{1}{(1+3y)}\,Na_2O \cdot yAl_2O_3 \rightarrow \frac{y}{(1+3y)}\,Al_2(SO_4)_3 + \frac{1}{(1+3y)}\,Na_2SO_4$$

The combination of these reactions gives the over-all reactions in Eq. [4.1] and [4.2].

In brief, (*i*) chemical reactions initiate at surface imperfections; (*ii*) since the degraded layer is porous, the reaction will continue to develop into the solid electrolyte, preferentially at these areas of imperfection; (*iii*) only the sulfates are thermodynamically stable corrosion products, while the O_2 and SO_3 are intermediate compounds during degradation.

β- or β″-alumina electrolytes, used in the as-sintered state, may be covered by a very thin, soda-rich, glassy surface film (5). Such a film would not be as stable as the crystalline electrolyte. Therefore, the reactions [4.1] and [4.2], are expected to be more favorable initially on the sintered surface compared to the polished surface from which such films have been removed.

Both experimental observations and thermodynamic calculations, summarized in Table II, indicate that the corrosion power of sodium polysulfide melts increases as the content of sulfur increases from Na_2S_2 to Na_2S_5, the normal composition range of a practical cell operation.

Influence of impurity contamination.—Oxygen.—With the participation of oxygen, the chemical reactions can be written as follows

$$O_2 + \frac{2(x-1)}{(3x+1)}\,Na_2O \cdot yAl_2O_3 + \frac{2}{(3x+1)}\,Na_2S_x \rightarrow \frac{2x}{(3x+1)}\,Na_2SO_4 + \frac{2y(x-1)}{(3x+1)}\,Al_2O_3 \qquad [4.4a]$$

$$O_2 + \frac{(x-1)}{2(3x+1)}\,Na_2O \cdot yAl_2O_3 + \frac{2}{(3x+1)}\,Na_2S_x \rightarrow \frac{(x-1)}{(3x+1)}\,NaAl(SO_4)_2 + \frac{2}{(3x+1)}\,Na_2SO_4 + \frac{(x-1)(y-1)}{2(3x+1)}\,Al_2O_3 \qquad [4.4b]$$

$$O_2 + \frac{[(3x-2)(x-1)+12y]}{6(3x+1)y}\,Na_2S_x + \frac{2(x-1)}{3(3x+1)y}\,Na_2O \cdot yAl_2O_3 \rightarrow \frac{2(x-1)}{3(3x+1)}\,Al_2(SO_4)_3 + \frac{(x-1)}{6y}\,Na_2S_{(x-1)} + \frac{[(x-1)+12y]}{6(3x+1)y}\,Na_2SO_4 \qquad [4.4c]$$

Obviously, these reactions are much more favorable thermodynamically in the presence of oxygen, since they have a large, negative $\Delta_rG°$, as shown in Table III. Experimental results agreed very well with this calculation. A significant reaction, evidenced by the deposition of corrosion products, and precipitation of crystallized products were found on the electrolyte surfaces when some free oxygen had been introduced into test tubes before sealing (see Fig. 3d and 4d). This further supports the assertion that the O_2 released during degradation is an intermediate product and will react further to produce sulfates.

Water.—When water has intercalated in the electrolyte, the reactions between polysulfides and the electrolyte changed and the corrosion products expected here were $NaHSO_4$ and NaOH, which could cause continued dissolution of the electrolyte

$$Na_2O \cdot yAl_2O_3 + \frac{x(3x-2)}{(4x-1)}\,Na_2S_x + \frac{(x-1)}{(4x-1)}\,H_2O \rightarrow \frac{(3x+1)x}{(4x-1)}\,Na_2S_{(x-1)} + \frac{x}{(4x-1)}\,NaHSO_4 + \frac{(x-2)}{(4x-1)}\,NaOH + yAl_2O_3 \qquad [4.5a]$$

If water and oxygen coexist, the reaction should be

Table III. The estimated standard free energies of the reactions between the electrolyte and $Na_2S_x(M)$ with impurity contaminations

Equation no.	x as in Na_2S_x	(kcal/mol O_2) $(\Delta_rG^\circ)_{350°C}$ β $y = 8$	β″ $y = 5.34$	$(\Delta_rG^\circ)_{400°C}$ β $y = 8$	β″ $y = 5.34$
Eq. [4.4a]	5	−91.6	−93.4	−90.4	−92.0
	4	−91.4	−93.1	−90.1	−91.6
	3	−91.5	−93.0	−90.2	−91.5
	2	−92.2	−93.3	−90.9	−91.8
Eq. [4.4b]	5	−82.8	−83.2	−80.0	−80.4
	4	−83.3	−83.7	−80.6	−81.0
	3	−84.5	−84.8	−81.9	−82.2
	2	−87.2	−87.5	−85.0	−85.2
Eq. [4.4c]	5	−579.3	−406.9	−574.3	−401.9
	4	−445.8	−319.6	−438.8	−313.4
	3	−314.1	−233.9	−306.5	−227.4
	2	−190.6	−154.2	−186.3	−150.2
		(kcal/mol H_2O) $(\Delta_rG^\circ)_{350°C}$		$(\Delta_rG^\circ)_{400°C}$	
Equation no.	x	β	β″	β	β″
Eq. [4.5a]	5	−4.2	−22.0	8.3	−7.1
	4	23.7	5.0	47.2	31.0
	3	52.9	32.4	81.5	63.7
	2	115.3	89.2	136.4	113.7
Eq. [4.5b]	5	−166.1	−168.9	−138.6	−141.0
	4	−181.7	−184.2	−152.0	−154.1
	3	−213.7	−215.6	−179.9	−181.6
	2	−311.8	−311.8	−265.9	−265.9
		(kcal/mol CO_2 or H_2O) $(\Delta_rG^\circ)_{350°C}$		$(\Delta_rG^\circ)_{400°C}$	
Equation no.	x	β	β″	β	β″
Eq. [4.6a]	5	−318.4		−301.0	
	4	−238.8		−225.1	
	3	−161.0		−151.5	
	2	−85.1		−80.0	
Eq. [4.6b]	5	−652.0	−635.7	−578.3	−581.5
	4	−537.1	−540.8	−472.3	−475.5
	3	−423.9	−427.6	−368.6	−371.8
	2	−312.6	−316.4	−267.0	−270.2
Eq. [4.6c]	5	−669.7	−676.2	−610.0	−615.7
	4	−548.9	−554.5	−493.4	−498.3
	3	−429.8	−434.4	−379.2	−383.2
	2	−312.6	−316.4	−267.0	−270.2
Eq. [4.6d]	5	−722.4	−737.4	−672.2	−685.1
	4	−584.0	−595.2	−534.9	−544.6
	3	−447.3	−454.8	−399.9	−406.4
	2	−312.6	−316.4	−267.0	−270.2

$$H_2O + \frac{(x-2)}{(x-1)} Na_2O \cdot yAl_2O_3 + \frac{1}{(x-1)} Na_2S_x + \frac{(3x+1)(x-2)}{(x-1)(2x-4)} O_2 \rightarrow \frac{x}{(x-1)} NaHSO_4 + \frac{(x-2)}{(x-1)} NaOH + \frac{(x-2)y}{(x-1)} Al_2O_3 \quad [4.5b]$$

The additional presence of oxygen makes the reactions possible, as it is evident in Table III.

Moist air.—If some O_2, CO_2, and H_2O are present by absorption from moist air, which is almost unavoidable, the following initial reactions are quite favorable, as follows from an examination of their Δ_rG° values listed in Table III

$$Na_2S_x + H_2O + CO_2 + \frac{3(x-1)}{2} O_2 \rightarrow Na_2CO_3 + H_2S + (x-1)\, SO_3 \quad [4.6a]$$

The H_2S and SO_3 can react further with the electrolyte to form sulfates: $NaHSO_4$, $Al_2(SO_4)_3$, $NaAl(SO_4)_2$, etc.

$$Na_2S_x + Na_2O \cdot yAl_2O_3 + \frac{(3x+1)}{2} O_2 + H_2O + CO_2 \rightarrow Na_2CO_3 + 2NaHSO_4 + \frac{(2-x+3y)}{3} Al_2O_3 + \frac{(x-2)}{3} Al_2(SO_4)_3 \quad [4.6b]$$

$$Na_2O \cdot yAl_2O_3 + \frac{2(3x+1)}{(x+2)} O_2 + \frac{4}{(x+2)} [Na_2S_x + H_2O + CO_2] \rightarrow \frac{4}{(x+2)} Na_2CO_3 + \frac{8}{(x+2)} NaHSO_4 + \frac{[x(y-1)+2(y+1)]}{(x+2)} Al_2O_3 + 2\frac{(x-2)}{(x+2)} NaAl(SO_4)_2 \quad [4.6c]$$

$$Na_2O \cdot yAl_2O_3 + \frac{(3x+1)}{2(x-1)} O_2 + \frac{1}{(x-1)} [Na_2S_x + H_2O + CO_2] \rightarrow \frac{1}{(x-1)} Na_2CO_3 + \frac{2}{(x-1)} NaHSO_4 + \frac{(x-2)}{(x-1)} Na_2SO_4 + yAl_2O_3 \quad [4.6d]$$

Coupled with oxygen or even carbon dioxide, which could come from the absorption of moist air on the electrolyte surface during cell construction, water does make the polysulfides more susceptible to corrosion. The possible reaction products now include $NaHSO_4$ and NaOH, whose melting points are 320° and 317°C, respectively. Thus, the presence of water can lead to an increased reaction of the electrolyte in the polysulfide melts at about 350°C (see Fig. 3e and 4e).

Fe-Ni-Cr and C.—An important aspect of sulfur side-degradation in practical Na/S cells is deposition of metal sulfides originating from container corrosion. The deposits formed on the electrolyte surface, as shown in Fig. 3c and 4c, have been identified as FeS_2, Cr_2S_3, Ni_3S_2, NiS_2, (Ni,Fe)S, and $NaCrS_2$, etc., and are similar to those reported by Park (11) and Battles (12). The possible reactions can be written as follows

$$Fe + 2Na_2S_x \rightarrow 2Na_2S_{(x-1)} + FeS_2 \quad [4.7a]$$

$$7Fe + 8Na_2S_x \rightarrow 8Na_2S_{(x-1)} + Fe_7S_8$$

$$3FeS_2 + 4SO_3 + 7Na_2S_x \rightarrow 3FeSO_4 + 7Na_2S_{(x+1)}$$

$$Ni + Na_2S_x \rightarrow Na_2S_{(x-1)} + NiS \quad [4.7b]$$

$$3Ni + 2Na_2S_x \rightarrow 2Na_2S_{(x-1)} + Ni_3S_2$$

$$2Cr + 3Na_2S_x \rightarrow 3Na_2S_{(x-1)} + Cr_2S_3 \quad [4.7c]$$

$$3Cr + 2C \rightarrow Cr_3C_2$$

$$7Cr + 3C \rightarrow Cr_7C_3$$

The reactions between the electrolyte and carbon have also been studied recently by Choudhury (3). The proposed reaction products include Na_2CO_3 and CO.

Dissolution/precipitation.—As shown in Fig. 5 and 6, after five weeks immersion, the sulfates produced by the reactions described above, had not yet saturated the Na_2S_x melts, and not much precipitation was found at that time. After 10 weeks immersion, however, the melts were saturated with the sulfates, and a lot of precipitation of crystallized products was found on all the surfaces of the electrolyte. The flower-like crystals, as clearly seen in Fig. 6, are believed to be sodium sulfates.

It appears, see Fig. 1 and 2, that more chemical reactions, deposition and or precipitation of corrosion products occurred in sulfur-rich melts, *i.e.*, Na_2S_5 and pure sulfur, and that more dissolution of corrosion products occurred in sulfur-poor melt, *i.e.*, Na_2S_2. This is perhaps due to the changes of the solubility of the sulfates in the sulfide melts as the composition of the sulfides changes.

Conclusions

Sodium β"-alumina electrolytes are chemically attacked by Na_2S_x melts and pure sulfur during immersion at high temperatures. The likely reactions can be written as described in Eq. [4.1]-[4.7], and occur preferentially on surface imperfections of the solid electrolyte.

The thermodynamically stable corrosion products are Na_2SO_4, $NaAl(SO_4)_2$, $Al_2(SO_4)_3$, $NaHSO_4$, Na_2CO_3, and NaOH. Most of these have high melting point and deposit on the electrolyte surface. Some have a low melting point and can be dissolved in the polysulfide melts, leading to dissolution or etching of the electrolyte surface.

There is a limited solubility of sodium sulfates in sodium sulfide melts. Precipitation of the crystallized sulfates occurred after prolonged exposure to sulfide melts and occurred preferentially at imperfections such as boundaries of large grains, or surface steps on the electorlyte surface.

The degree of corrosion increased as the content of sulfur increased in the range of Na_2S_2 to Na_2S_5 to sulfur.

In addition to the reactions between the electrolyte and Na_2S_x or sulfur, the corrosion products of transition metals, and current collector material (graphite), also deposit on the electrolyte surface.

All of the corrosion reactions were greatly accelerated by contaminations of impurities, such as water and oxygen, and transition metals.

In a practical cell, the environment that the electrolyte will be exposed to is expected to be a combination of the above situations to some degree. The degraded layer formed on electrolyte surfaces in an actual Na/S cell would be expected to be a mixture of (*i*) sulfates and carbonates, produced by reactions [4.1] through [4.6], and (*ii*) corrosion products of cell parts, by reactions [4.7]. This layer may block sodium-ion transport, cause inhomogeneous current distribution, and could spall off when new compounds form underneath it, leading to a progressive degradation of positive electrode contact interface of the electrolytes.

Since the corrosive power of the polysulfide melts increases at a composition corresponding to the fully charged state and is enhanced for free sulfur, it would seem advisable to avoid heterogeneous electrode reactions that expose the electrolyte surface for unnecessarily long periods to the most corrosive sulfide melts that may occur at the end of charge.

Acknowledgments

The authors wish to thank Dr. S. Visco for valuable discussions and suggestions. This work was supported by the U.S. Department of Energy under contract no. DE-AC03-76SF00098.

Manuscript submitted July 7, 1986; revised manuscript received Aug. 12, 1987.

Lawrence Berkeley Laboratory assisted in meeting the publication costs of this article.

REFERENCES

1. L. C. De Jonghe, L. Feldman, and A. Buechele, *Solid State Ion.*, **5**, 267 (1981).
2. L. C. De Jonghe, L. Feldman, and A. Buechele, *J. Mater. Sci.*, **16**, 780 (1981).
3. N. S. Choudhury, *This Journal*, **133**, 425 (1986).
4. M. L. Miller, B. J. McEntire, G. R. Miller, and R. S. Gordon, *Am. Ceram. Soc. Bull.*, **58** (5), 522 (1979).
5. R. N. Singh, *ibid.*, **67** (10), 637 (1984).
6. J. T. Kummer, "Progress in Solid State Chemistry," Vol. 7, H. Reiss and J. O. McCaldin, Editors, pp. 141-175, Pergamon Press, Inc., New York (1972).
7. M. Itoh, K. Kimura, and Z. Kozuka, *Trans. Jpn. Inst. Met.*, **26**, 353 (1985).
8. N. K. Gupta and R. P. Tischer, *This Journal*, **119**, 1033 (1972).
9. The NBS Tables of Chemical Thermodynamic Properties, *J. Phys. Chem. Ref. Data*, **11**, Suppl. no. 2 (1982).
10. "JANAF Thermochemical Tables," 2nd ed., U.S. Department of Commerce, National Bureau of Standards, Vol. 37, (1971, 1978); *J. Phys. Chem. Ref. Data*, **11** (3) (1982).
11. D.-S. Park, Proceedings of DOE/EPRI Beta (Sodium-Sulfur) Battery Workshop V, EPRI EM-3631-SR, pp. 6-191 (1984).
12. J. E. Battles, Proceedings of DOE/EPRI Beta (Sodium-Sulfur) Battery Workshop V, EPRI EM-3631-SR, pp. 6-291 (1984).

Development of Low Chromium Substitute Alloys for High Temperature Applications

Je M. Oh*

United States Department of the Interior, Bureau of Mines, Albany Research Center, Albany, Oregon 97321

ABSTRACT

The oxidation of a base-line Fe-8Cr-16Ni (weight percent) composition was compared to that of alloys with small additions of Al, Si, Mo, and Mn. Oxidation was done in air over the temperature range of 600°-1000°C for up to 1000h. Alloys that contained Al and Si showed excellent oxidation resistance because of the formation of a layer containing Si at the scale-metal interface. Small additions of Al seemed to form oxide nuclei during a transient oxidation period, aided the formation of a layer containing Si and/or a chromium oxide, and provided better oxide adherence. Molybdenum and manganese additions stabilized a fully austenitic microstructure at room temperature. The oxidation behavior of these alloys was compared to that of 304 stainless steel and some commercial superalloys. Reaction kinetics, oxide morphologies, and oxidation mechanisms of the substitute alloys are described.

One of the Bureau of Mines research goals is to minimize the requirement for domestically scarce minerals through substitution and conservation. Chromium, in particular, is the element which provides the characteristics of oxidation and corrosion resistance to stainless steels (SS) by forming a protective chromium oxide scale. Because the United States has no commercial chromium deposits, chromium is considered to be a particularly vulnerable strategic metal. Therefore, there is interest in developing low chromium alloys that could substitute for stainless steels in some applications. A significant fraction of the stainless steel used in the United States is used in applications where resistance to high temperature oxidation is important.

*Electrochemical Society Active Member.